Inorganic Chemistry

Article

pubs.acs.org/IC

Stabilizing Alginate Confinement and Polymer Coating of CO-Releasing Molecules Supported on Iron Oxide Nanoparticles To Trigger the CO Release by Magnetic Heating

Hajo Meyer,[†] Felix Winkler,[†] Peter Kunz,[†] Annette M. Schmidt,[‡] Alexandra Hamacher,[§] Matthias U. Kassack,[§] and Christoph Janiak*[,†]

[†]Institut für Anorganische Chemie und Strukturchemie, Universität Düsseldorf, 40204 Düsseldorf, Germany

[‡]Institut für Physikalische Chemie, Universität zu Köln, Luxemburger Str. 116, 50939 Köln, Germany

[§]Institut für Pharmazeutische und Medizinische Chemie, Universität Düsseldorf, 40204 Düsseldorf, Germany

Supporting Information

ABSTRACT: Maghemite (Fe_2O_3) iron oxide nanoparticles (IONPs) were synthesized, modified with covalent surface-bound CO-releasing molecules of a tri(carbonyl)-chlorido-phenylalaninato-ruthenium(II) complex (CORM), and coated with a dextran polymer. The time- and temperature-dependent CO release from this CORM-3 analogue was followed by a myoglobin assay. A new measurement method for the myoglobin assay was developed, based on confining "water-soluble" polymer-coated Dextran500k@CORM@IONP particles in hollow spheres of nontoxic and easily prepared calcium alginate. Dropping a mixture of Dextran500k@CORM@IONP and sodium alginate into a $CaCl_2$ solution leads to stable hollow spheres of Ca^{2+} cross-linked alginate which contain the Dextran500k@CORM@IONP particles. This "alginate-method" (i) protects CORM-3 analogues from rapid CO-displacement reactions with a protein, (ii) enables a spatial separation of the CORM from its surrounding myoglobin assay with the alginate acting as a CO-permeable membrane, and (iii) allows the use of substances with high absorptivity (such as iron oxide nanoparticles) in the myoglobin assay without interference in the optical path of the UV cell. Embedding the CORM@IONP nanoparticles in the alginate vessel represents a compartmentation of the reactive component and allows for close contact with, yet facile separation from, the surrounding myoglobin assay. The half-life of the CO release from Dextran500k@CORM@IONP particles surrounded by alginate was determined to be 890 ± 70 min at 20 °C. An acceleration of the CO release occurs at higher temperature with a half-life of 172 ± 27 min at 37 °C and 45 ± 7 min at 50 °C. The CO release can be triggered in an alternating current magnetic field (31.7 kA m^{-1}, 247 kHz, 39.9 mT) through local magnetic heating of the susceptible iron oxide nanoparticles. With magnetic heating at 20 °C in the bulk solution, the half-life of CO release from Dextran500k@CORM@IONP particles decreased to 155 ± 18 min without a noticeable temperature increase in the dispersion. At 37 and 50 °C, the half-life for the CO release triggered by local magnetic heating was 65 ± 5 min and 30 ± 3 min, respectively. Thus, at a physiological temperature of 37 °C, magnetic heating accelerates the CO release of the IONP-bound CORM by a factor of ~2.6. The activation energy for CO release from a CORM-3 analogue was determined to be E_A = 78 kJ/mol.

INTRODUCTION

Ever since the physiological effect of carbon monoxide (CO) on the human body was first described by John Haldane in 1927, the molecule has been viewed as a "silent killer".[1] CO hinders the oxygen transport in the blood system, because it occupies the oxygen binding site in hemoglobin. This effect is based on the about 245-fold stronger binding constant of the CO-heme iron complex in comparison to the O_2 hemoglobin adduct. Even small quantities of CO in the surrounding air (about 100 ppm) can be potentially harmful to the human body.[2,3] The gas itself is both color- and odorless.

However, every cell in mammalian and, thereby, also human organisms expresses *heme oxygenase* enzymes,[4] which are capable of producing carbon monoxide continuously in order to regulate the circadian rhythms, memory, and hemodynamics.[5−7] The gas can be classified as a small molecule messenger like nitrogen oxide (NO) and hydrogen sulfide (H_2S), which regulate various processes through biochemical signaling cascades.[6,8−10]

Because of the regulatory and cytoprotective effects of CO, it has already been extensively investigated for medical applications.[6] The administering of gaseous CO was successfully tested in the human body. It features a half-life of 3−7 h and was well tolerated at 3 mg per kg for 1 h. The gas bound reversibly to cellular targets, and lung exhalation was determined to be the only way for CO to exit mammal bodies in this therapeutic approach.[6,11] Positive effects on many diseases such as tumor or carcinoma growth, malaria, bacterial infections, pulmonary fibrosis, rheumatoid arthritis, acute liver

Received: July 24, 2015
Published: November 23, 2015

DOI: 10.1021/acs.inorgchem.5b01675
Inorg. Chem. 2015, 54, 11236−11246

failure, thermal injury, asthma, or sickle cell disease have been reported.[12,13] However, when CO is administered as a gas, it is difficult to accumulate it in a specific site (e.g., tumor or burned skin). In fact, the gas also reaches healthy tissue and the dose needs to be relatively high in order to achieve an effect on diseased sites. In addition, the quantity needs to be carefully controlled and special administering equipment is necessary.

For specific targeting of diseased tissue in the body, "solid carbon monoxide"—small molecules that are able to release carbon monoxide—were investigated. The first so-called CORMs (CO-releasing molecules) studied for this purpose were $Fe(CO)_5$, $Mn_2(CO)_{10}$ (CORM-1), and $[Ru(CO)_3Cl_2]_2$ (CORM-2) (Figure 1).[14,15]

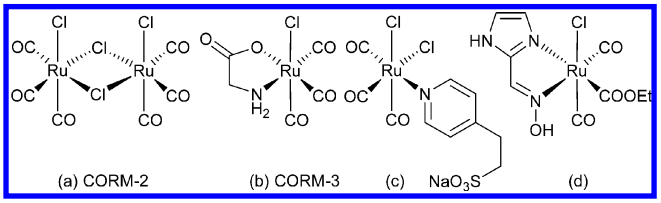

Figure 1. Examples of ruthenium-based CO-releasing molecules (CORMs) for biological investigations: (a) CORM-2,[15] (b) CORM-3,[14] (c) $Ru(CO)_3Cl_2(4\text{-}NC_5H_4(CH_2)_2SO_3Na)$,[16] (d) Ru(imidazole-2-carbaldehyde oxime)$(COOMe)(CO)_2Cl$.[17]

However, these first CORMs were hardly water-soluble and released CO way too fast for a precise administering (half the gas load in less than 1 min at physiological conditions[15]). In 2003, Motterlini and co-workers,[3,18] introduced the water-soluble complex $[Ru(CO)_3(glycinate)]$ (CORM-3) (Figure 1), which released CO under physiological conditions[14] and showed vasodilatative, anti-inflammatory, renoprotective, and antiapoptosis effects in preclinical studies.[19] In the last 10 years, Ru-based CORMs became a very important field of research with several studies of CORM-2 and the water-soluble CORM-3.[6,14,15] Different CORMs with ruthenium carbonyl are known, and the number is still increasing (Figure 1).[16,17]

The half-life of CO release for CORM-3 via a pseudo-first-order reaction is 1 min at 37 °C in PBS buffer,[20] 2.3 min at 30 °C in PBS buffer,[21] and 3.6 min in human plasma,[22] apparently due to CO abstraction by heme proteins.[23] Different possible medical applications of CORMs may require CORMs with different release kinetics. In addition, CORMs may also induce effects due to their Ru-containing moieties.[24,25]

Recent studies presented CORMs which liberate CO upon external stimuli like change in pH,[26,27] increasing temperature, UV irradiation,[28,29] and oxidative or enzymatic degradation.[30] The immobilization of CORMs in[31] and on[32,33] polymer materials may open a door for new aspects in medicinal chemistry.[34,35] Drugs which are conjugated to polymers are limited to the vascular system and can be transported directly to the target area. A passive accumulation of macromolecular systems in tumor tissues due to the so-called enhanced permeability and retention (EPR) effect was first described and investigated by Maeda et al.[36,37]

The growth of tumors (>2 mm) is ensured by fast growing blood vessels to supply nutrients and dioxygen. The blood vessels are destabilized due to vascular endothelial growth factors (VEGFs) into the extracellular space and have a higher permeability than normal grown blood vessels.[38] The resulting blood vessels are lacking the tight junctions that are normally present between adjacent vascular endothelial cells, which leaves holes on an order of magnitude larger than normal vascular pores (healthy tissue has pores of 5−8 nm; tumor tissue can have pores of about 50 nm, and interendothelial junctions of about 500 nm). The EPR effect refers to the property of these large pores to allow polymers to enter the tumor interstitium and to remain and accumulate there because the polymers are not removed by the lymphatic system.[39] The accumulation of functionalized polymers in tumor tissue with the ability to release CO is an additional concept of constructing polymer-CORM conjugates. In such conjugates, the use of a slow CO releaser from which the CO release can be triggered or activated by magnetic heating through alternating magnetic field should be of interest.

In our previous work, we presented a new concept of controlled CO release by attaching the CO-releasing molecule to the surface of iron oxide nanoparticles (**3** in Figure 2), which

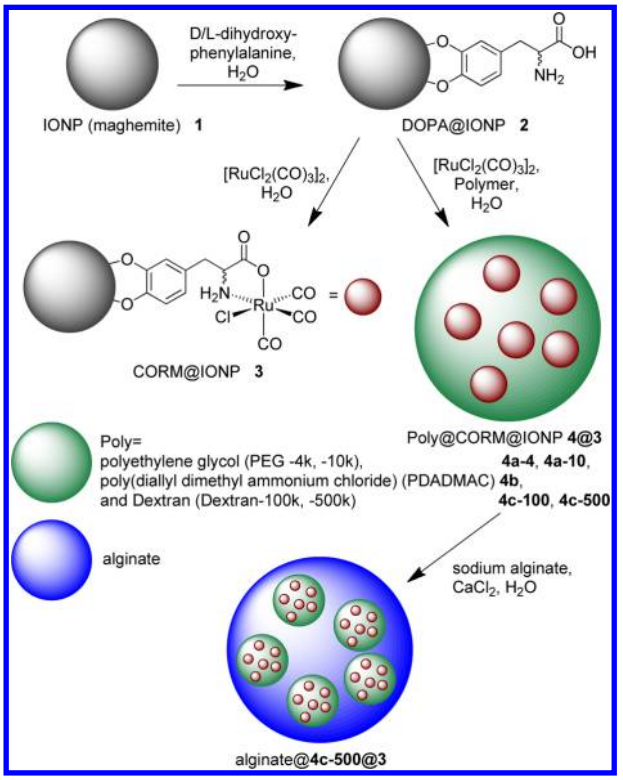

Figure 2. Synthesis of CORM-functionalized iron oxide nanoparticles, without polymer coating (**3**) and with polymer coating (**4**). Formation of the alginate@**4c-500@3** spheres for myoglobin assay measurements.

are susceptible to local heating through an external alternating current magnetic field.[40] The application of such an external alternating magnetic field yielded an increase in CO-release rate by a factor of 2 with a half-life of 7 ± 2 min (down from 13 ± 2 min) at 25 °C in a buffered myoglobin-assay solution.

The triggered CO release from an otherwise stable CORM is a main target in our work. Therefore, we needed to decrease the still too fast rate of CO release at room temperature. In addition, the CORM@IONP system **3** still has a low water solubility and a relatively fast CO release, especially in the presence of the heme protein myoglobin. Both properties limit possible medical applications. Hence, we sought to increase water solubility together with kinetic stability of the CORM@IONP dispersion. In order to prevent CO abstraction by heme

DOI: 10.1021/acs.inorgchem.5b01675
Inorg. Chem. 2015, 54, 11236−11246

proteins, a polymer coating of the CORM@IONP (**3**) dispersion was envisioned, which should also enhance the water solubility. At the same time, the strong absorptivity of the black IONP dispersion hampers CO-release studies through the myoglobin assay in the same dispersion. The CO release is followed by UV/vis spectrometry. Therefore, we describe here the alginate confinement of "water-soluble" Poly@CORM@IONP (**4@3**) particles (Figure 2) with high kinetic stability due to spatial separation of the surrounding myoglobin assay.

RESULTS AND DISCUSSION

The maghemite nanoparticles (IONP) **1** and their dopamine surface functions (DOPA@IONP) **2** (cf. Figure 2) were prepared by a known procedure.[40] The CORM-3 analogous Ru-carbonyl complex on the dopamine-functionalized IONPs (CORM@IONP, **3**, Figure 2) and the polymer coating of CORM@IONP were obtained in a simple mixing reaction. For the coating of the CORM@IONP particles, the polymers Poly-Ethylene-Glycol (PEG-4k, -10k), Poly-Di-Allyl-Di-Methyl-Ammonium-Chloride (PDADMAC), and Dextran (Dextran-100k, -500k) (Figure 3) were investigated. Polymer coatings are

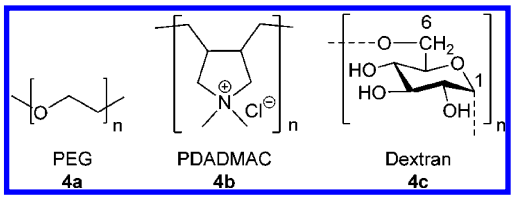

Figure 3. Repeat units of used polymers from left to right: **P**oly-**E**thylene-**G**lycol (PEG, **4a**), **P**oly-**D**i-**A**llyl-**D**i-**M**ethyl-**A**mmonium **C**hloride (PDADMAC, **4b**), and Dextran (**4c**).

capable of excluding water from the magnetic core, restricting the diffusion of water molecules, and increasing the residence time of water molecules by forming hydrogen bonds. Thus, they influence the solubility of the functionalized nanoparticles.[41]

PEG is the polymer most commonly used to stabilize nanoparticles for medical applications.[42] A PEG coating interacts with the particle via hydrogen bonds and van der Waals forces of the polymer to the hydroxyl groups on the IONP. The PEG-coated particles **4a-4@3** and **4a-10@3** were completely insoluble in aqueous media. PDADMAC has been reported to stabilize various nanoparticles in aqueous media.[43] The polycation probably forms hydrogen bonds and ionic interactions with the CORM-functionalized particle. The PDADMAC coating in **4b@3** provided the best water solubility of all polymers screened. Dextran has also been studied extensively for polymer coatings of maghemite nanoparticles in medical applications such as MRI or tumor treatment.[44,45] The interaction between the nanoparticle and the polymer is noncovalent. Both Dextran-coated composites **4c-100@3** and **4c-500@3** formed very fine dispersions in aqueous media.

The composite compound **4@3** was precipitated with acetone, washed with acetone, vacuum-dried, and analyzed by IR spectroscopy (Table S1, Figures S2a and S2b, Supporting Information).

The CO stretching vibrations of the $Ru(CO)_3$-fragment in **4c-500@3** were observed around 1992 and 2063 cm^{-1} (see the Supporting Information), which agree with the vibrational frequencies of the analogous CORM-3 and the model compound $PhCH_2CH(NH_2)CO_2RuCl(CO)_3$ (see Figure S1) under basic conditions.[40]

From Ru elemental analysis by flame AAS together with the determination of the absolute amount of CO released, we estimate a loss of 0.20(5) mol of carbon monoxide per mol of Ru from alginate@**4c-500@3** in the myoglobin assay. For CORM-3, 1 mol of CO per mol of Ru can be released. After the release of one CO from CORM-3, an inactive form, termed iCORM, is formed. The inactive iCORM form of CORM-3[14] is not able to release further CO after the loss of one CO. The low CO amount per Ru in our case might be the result of a previous loss of CO during the synthesis. Thus, the low intensity band at ~2130 cm^{-1} for the Ru-CORM in Dextran@CORM@IONP (**4c-500@3**) (Figure 2b in the Supporting Information) is in agreement with the found low amount of CO which can still be released from the composite alginate@**4c-500@3**. It is known from the very recent literature that CORM-2 will lose 1.8 CO equivalents as CO_2 in water within 24 h.[16]

The CO release was followed by the well-known myoglobin assay using UV/vis spectroscopy (see the Supporting Information). For Poly@CORM@IONP, **4@3**, a single-step pseudo-first-order CO release can be deduced without a magnetic field from the relative decrease and increase in the absorption bands at 541, 556, and 578 nm.

We observed half-lives of the CO release at 37 °C for CORM@IONP **3** of 9 ± 1 min and an increase upon polymer coating with PEG-4k (**4a-4@3**) to 11 ± 1 min, PEG-10k (**4a-10@3**) to 11 ± 1 min, PDADMAC (**4b@3**) to 11 ± 0.1 min, Dextran 100k (**4c-100@3**) to 17 ± 1 min, and Dextran 500k (**4c-500@3**) to 32 ± 2 min (Figure 4). The remarkably long

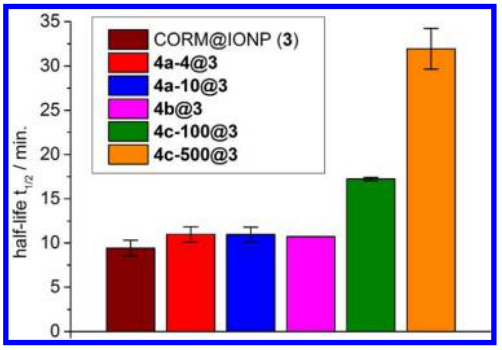

Figure 4. Determined half-lives of the CO release from CORM@IONP (**3**, $t_{1/2}$ = 9 ± 1 min) and the polymer-coated CORM@IONPs **4a-4@3** (PEG-4k, $t_{1/2}$ = 11 ± 1 min), **4a-10@3** (PEG-10k, $t_{1/2}$ = 11 ± 1 min), **4b@3** (PDADMAC, $t_{1/2}$ = 11 ± 0.1 min), **4c-100@3** (Dextran-100k, $t_{1/2}$ = 17 ± 1 min), and **4c-500@3** (Dextran-500k, $t_{1/2}$ = 32 ± 2 min) at 37 °C.

half-life of **4c-500@3** is probably due to the high molecular weight of the polymer, leading to very long chains and possibly hyperbranching, which allows for an effective coverage of the CORM@IONP particles. Thus, the substitution of exchangeable ligands like CO in the CORM-3 derivative upon interaction with the myoglobin protein is suppressed and the half-life is increased.

The amount of ruthenium in the **4c-500@3** composite was determined with atom absorption spectroscopy (AAS) to an average of 0.33 wt % ruthenium (3.3 mg Ru/g composite) (see the Experimental Section or the Supporting Information for details). The molar Ru:Fe ratio in the sample Dextran@

DOI: 10.1021/acs.inorgchem.5b01675
Inorg. Chem. 2015, 54, 11236−11246

CORM@IONP (**4c-500@3**) was determined by AAS for both elements to be 1:48. This is less ruthenium compared to our previous publication on CORM@IONP (Ru:Fe 1:25).[40] The difference is probably a result of using deionized water for the synthesis of **4c-500@3** instead of methanol as for CORM@IONP in our previous work.[40] It is now known from the very recent literature that CORM-2 will lose 1.8 CO as CO_2 in water within 24 h.[16] However, water had to be chosen in this work to increase the dispersibility of the DOPA@IONP and CORM@IONP intermediates and to form the composite alginate spheres. The synthesis of CORM@IONP in methanol led to highly agglomerated large particles, which did not lend itself anymore to be coated by a polymer shell.[40]

Dispersions of IONPs (**1**) yield a hydrodynamic diameter in the range of 10−30 nm with an average diameter of 12 ± 4 nm (standard deviation σ) from dynamic light scattering (DLS) investigations (Figure 5). The DOPA@IONP nanoparticles **2**

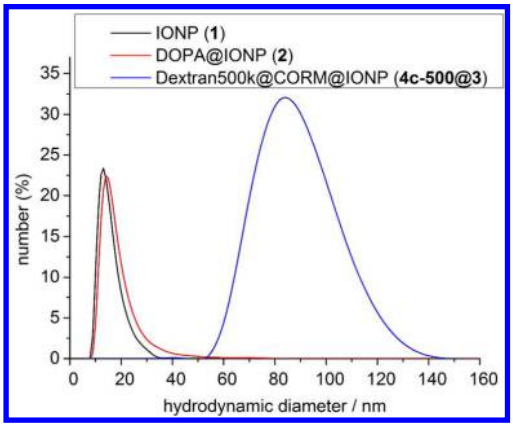

Figure 5. Size distribution of the hydrodynamic diameter of the IONP, **1** (black), DOPA@IONP, **2** (red), and Dextran500k@CORM@IONP, **4c-500@3** (blue), particles in water (1 mg/mL) from dynamic light scattering (DLS) investigations. The CORM-functionalized maghemite-NPs, **3**, could not be efficiently dispersed anymore in water for a DLS measurement.[40]

have a broader diameter distribution of 10−50 nm with an average of 14 ± 4 nm, in agreement with their modified surface and the increased hydrodynamic diameter. The **4c-500@3** composite particles gave an even wider size distribution in the range of 60−140 nm with an average diameter of 85 ± 15 nm (Figure 5). This large increase in size and size distribution for **4c-500@3** is ascribed to the incorporation of several CORM@IONPs particles within the same polymer sphere (cf. TEM pictures in Figure 6 and Figure S3a).

High-angle annular dark-field scanning transmission microscopy (HAADF-STEM) supports the diameter range of the **4c-500@3** composite from the DLS measurement. Even at high dilution of the coated CORM@IONPs (**3**), the TEM analysis only showed ensembles of agglomerated iron oxide particles (Figure 6 and Figure S3a). Although the organic dextran polymer is not seen in the TEM, this suggests that several nanoparticles **3** are collected within a polymer sphere. In these ensembles, the CORM@IONPs had a diameter range of 5−12 nm, average of 9 ± 1 nm, which agrees well with the average TEM diameter of bulk **3** of 9 ± 2 nm.[40] The TEM diameter is expected to be slightly smaller than the hydrodynamic diameter from DLS, which could only be measured for DOPA@IONP (**2**) (14 ± 4 nm) as the CORM@IONPs (**3**) could not be well dispersed in water anymore. From TEM, the ensembles of

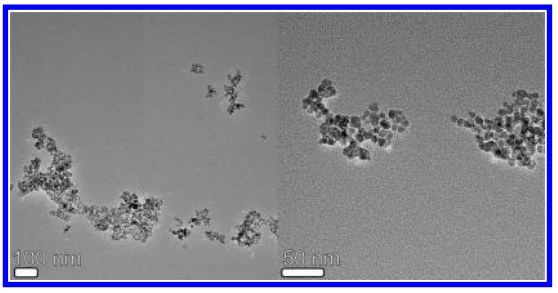

Figure 6. TEM pictures of **4c-500@3** showing ensembles of agglomerated CORM@IONPs (**3**). Even with high dilution, a separation of the polymer-coated nanoparticles on the grid could not be achieved, which indicates the assembly of several nanoparticles **3** within a polymer sphere. The surrounding polymer sphere of the nanoparticles cannot be seen due to the low resolution and much lower contrast of the polymer compared to the iron oxide nanoparticles. See the Supporting Information (Figure S3a) for additional TEM pictures.

these agglomerated particles have estimated sizes from 50 to 120 nm (and more; see histogram in Figure S3a), which is slightly smaller but thereby matches the hydrodynamic diameter range of **4c-500@3** from DLS in Figure 5. By comparison, bulk maghemite IONPs **1** can be well distributed on the grid without showing agglomerated ensembles (see TEM pictures in Figure S3b in the Supporting Information). From TEM, these bulk IONPs have a very small size distribution of 8 ± 1 nm in a range of 5−12 nm similar to the DLS curve for **1** in Figure 5.

A temperature-dependent CO release of the **4c-500@3** composite was followed by a myoglobin assay and showed the desired kinetic stabilization with a decrease of the CO-release rate (Figure 7). We had found a half-life of 13 ± 2 min for the

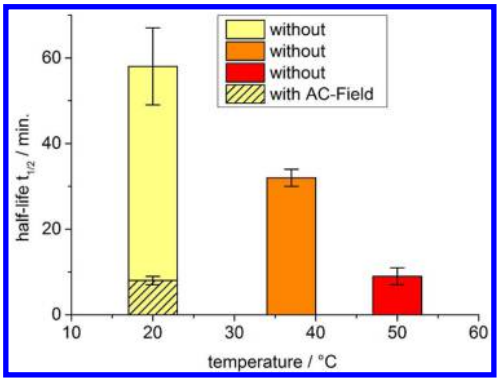

Figure 7. Half-life of CO release for **4c-500@3** at different temperatures, determined with a myoglobin assay.

CO release from CORM@IONP (**3**) at 25 °C[40] and observed for **4c-500@3** half-lives at 20 °C of 58 ± 9 min, at 37 °C of 32 ± 2 min, and at 50 °C of 9 ± 2 min (Figure 7). The application of an external alternating magnetic field (31.7 kA m^{-1}, 247 kHz, 25 °C, 1.7 mT) triggered the CO release through local heating of the maghemite IONP. Such a local magnetic heating yielded a 5 to 6-fold accelerated CO release with a half-life of 8 ± 1 min at 20 °C compared to 58 ± 9 min without the magnetic field at the same temperature (Figure 7).

Still, it was not easy to follow the CO release over time with the myoglobin assay due to the strong UV/vis absorption of the dark iron oxide nanoparticles in the dispersion (Figure S4 in the Supporting Information). A stable **4c-500@3** dispersion in

DOI: 10.1021/acs.inorgchem.5b01675
Inorg. Chem. 2015, 54, 11236−11246

aqueous solution is advantageous for the intended medical application in body fluids. However, the dark color of the dispersion from the iron oxide nanoparticles strongly increases the spectral noise and, thereby, masks the changes in absorption of the myoglobin when binding the CO (Figures S6–S8). We rely on clearly detectable time-dependent UV/vis absorption differences for the *in vitro* CO-release studies to accurately determine the half-life. Hence, it is necessary to separate the dark **4c-500@3** composite from the myoglobin assay for accurate time-dependent release studies. Some methods were already described to separate the solution of the myoglobin assay from the CORM solution where the CO release occurs.[35] Motterlini presented a construction of two separated chambers connected via an Anapore membrane through which only the CO can permeate. The membrane is expensive, and the whole system is not temperature controllable. Time-dependent measurements were only possible if samples were taken from and transferred back into the cell.[15]

We wanted to avoid a time delay through long diffusion paths of the CO from the CORM to the myoglobin phase. We also aimed for a system, which can be used in a single and normal cuvette cell in any commercial UV/vis spectrometer. Therefore, we intended to develop an inexpensive and easy method for the widely accepted myoglobin assay which also would divide the two reaction phases, but still retain them in one temperature controllable cell for the absorption measurement. The resolution of the UV/vis measurement should only be limited by the recording speed of the spectrometer to achieve a continuous and not interrupted measurement.

Such a compartmentation would also be relevant to highly colored metal-carbonyl compounds, which is usually the case with photolabile CORMs. Such photo-CORMs often overlap in their absorption bands with myoglobin, and also the CO-deficient reaction product, the iCORM (inactivated CORM), can be colored. In such a case, complicated spectral deconvolution techniques are required to derive at the half-life for the CO release through the myoglobin assay.[35,46,47]

We have presented here a CORM-modification to use the established myoglobin assay in order to monitor CO release with little interference. For a balanced discussion, we also want to point to other available methods and their (dis-)advantages.

Electrochemical sensors do not need anaerobic conditions and can measure the CO concentration directly in the solution, but they only provide a limited view of the release of carbon monoxide.[48] Further studies of the influence from electrochemical reactions to the CO release have not been done yet. Anyway, the use of metallic sensors for an online CO-release measurement in an alternating magnetic field is not reasonable.

Fluorescent probes for the detection of CO can detect CO in lower concentrations than the myoglobin assay. However, the response time of the probe is relatively long and not applicable for short time kinetic measurements.[49,50]

Gas-phase IR spectroscopy provides a very sensitive and high-resolution method for measuring the CO release from various compounds in the gas phase or in solution (ATR technique). It is independent of any additional additives (e.g., buffer or sodium dithionite reductant) and, therefore, very interesting.[48] Yet, for our study of the alternating magnetic field effect, the construction of a temperature controllable IR chamber, which fits into the available AC field coil, was seen as very demanding, so we opted for the more feasible UV–vis cuvette with the Mb assay.

Gas chromatography could be used with different detectors like GC-RGD,[51] GC-MS,[52] or GC-TCD. The latter is, however, not capable of continuous measurements as samples have to be taken from the reaction mixture or the headspace of the solution.[48]

The presented encapsulation method with alginate accepted the disadvantages of the myoglobin assay (e.g., sodium dithionite) but presented a novel approach to minimize the disadvantage of strong absorbing substances to compare their behavior with the results of the often used myoglobin assay.

Sodium alginate is an anionic polysaccharide, which is distributed widely in cell walls of brown algae. The linear copolymer consists of ß-D-mannuronate and α-L-guluronate blocks or sequences (Figure S9). A supramolecular cross-linkage of the deprotonated carboxylate groups forms with Ca^{2+} ions by Coulomb interactions.[53,54] Dropping a solution of the substrate and sodium alginate into a solution of calcium ions rapidly forms hollow spheres of calcium cross-linked alginate which incorporate the **4c-500@3** substrate. Nearly complete incorporation of the **4c-500@3** particles inside the alginate spheres is evident from the decolorization of the initial dispersion (Figure 8).

Figure 8. (a) **4c-500@3** dissolved in water, (b) solution of sodium alginate with **4c-500@3** in water, and (c) alginate spheres formed from dropping the solution (b) into a calcium chloride solution.

The Ca-alginate (Figure S9) presents a porous membrane that still allows smaller molecules like solvent to permeate but retains nanoparticles. Hence, we formed in situ a container for the **4c-500@3** material. This method is simple and requires no heating which otherwise can be a problem to temperature-sensitive samples like CORMs. Alginate is not toxic and already in use for biomedical applications[55] like cell encapsulation,[56,57] as well as in the molecular kitchen.[58] Even the insertion of metal–organic framework particles has been described in the literature.[59]

We found that alginate spheres form readily by dropping a mixture of **4c-500@3** and sodium alginate in doubly deionized water into a calcium chloride solution (Figure 8). We performed the alginate enclosure with several different nanoparticles from their aqueous dispersion for maghemite-IONP **1**, DOPA@IONP **2**, and gold nanoparticles (Figure S10 in the Supporting Information). The magnetism of the **4c-500@3** composite or basic iron oxide nanoparticles **1** is retained in the alginate spheres so that the alginate spheres can be readily collected or arranged and manipulated with an external magnetic field (Figure 9).

The alginate spheres assume a diameter of around 1–2 mm and carry an amount of approximately 0.06 mg **4c-500@3** per sphere with the described synthesis. Hence, the total volume of the spheres is around 10 μL, the same volume as a drop of alginate solution from a Braun 0.60 × 80 mm BL/LB syringe

DOI: 10.1021/acs.inorgchem.5b01675
Inorg. Chem. 2015, 54, 11236–11246

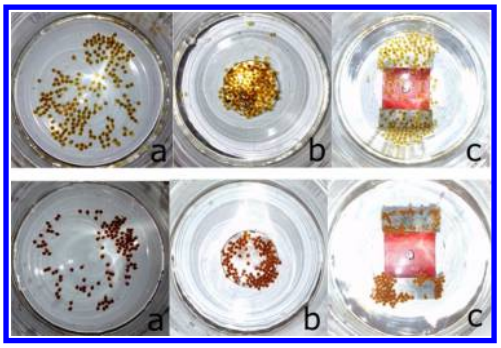

Figure 9. Alginate@**4c-500@3** (top) spheres and alginate@**1** (bottom) and their arrangement in magnetic fields: (a) No magnet, (b) round magnet, and (c) bar magnet under the glass vessel.

needle with 2 mm in diameter. The formed spheres can be collected and separated with a magnet. The spheres were washed and stored in 3-(*N*-morpholino)propanesulfonic acid buffer (MOPS buffer) for a maximum time of 6 h before the CO-release measurements so as to avoid aging effects and to ensure reproducible results. The spheres can easily be transferred into a UV/vis cuvette and fixed with a permanent magnet at the bottom of the cuvette. UV absorption measurement is possible in the central section of the cell without any interference from absorption of the nanoparticles in the optical path (Figure 10a). A maximum amount of around 15 spheres can be collected in the lower part of a thermostated UV/vis cuvette with an inner cross section of 5 × 10 mm (Figure 11a,b).

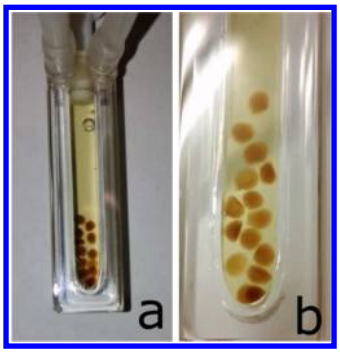

Figure 10. Thermostated UV/vis cell with 15 alginate@**4c-500@3** spheres in a yellow-colored myoglobin assay before triggering the CO release. In the left cell (a), the 15 alginate spheres are partly lying behind each other in the bottom of the cell. The right cell (b) was laid down so that almost all the alginate sphere could be spread apart, with only two spheres just behind each other.

For the alginate@**4c-500@3** composite, the CO release was again followed with a myoglobin assay in a thermostated cuvette (Figure 10) using UV/vis spectroscopy without and with alternating current (AC) magnetic field (Figure 11; see the Supporting Information for details). All measurements were done three times and show a reproducible half-life of 890 ± 70 min at 20 °C, 172 ± 27 min at 37 °C, and 45 ± 7 min at 50 °C (Figure 12). In the presence of the AC magnetic field, that is, with magnetic heating, the half-life is lowered to 155 ± 18 min at 20 °C, to 65 ± 5 min at 37 °C, and to 30 ± 3 min at 50 °C (Figure 12). Reduction of the half-life upon heating of the IONP in the alternating magnetic field is more pronounced at lower temperatures, as shown in Figure 12. We think that these results show conclusively (i) the capability to trigger the CO release from CORMs on magnetic nanoparticles by magnetic heating and (ii) the possibility to effectively stabilize the reactive CORM-3 system in a water-soluble polymer shell. Without such protection, CORM-3 reacts within minutes with heme proteins to yield protein-Ru$(CO)_2$ adducts by eliminating all non-CO ligands from CORM-3 in addition to one CO ligand, which is released in the form of CO_2.[23]

The amount of CO released was determined with the Lambert−Beer law and calculated to be 0.20(5) mol of carbon monoxide per mol of Ru from alginate@**4c-500@3** in the myoglobin assay. For a CORM-3 analogue, 1 mol of CO per mol of Ru should be released. However, we have synthesized DOPA@IONP (**2**) and Dextran@CORM@IONP (**4c-500@3**) (cf. Figure 2) in water to avoid agglomeration of the DOPA@IONP and CORM@IONP intermediates. It is now known and quantified from the recent literature that CORM-2 will lose 1.8 CO equivalents as CO_2 in water within 24 h.[16]

The half-life of the molecular CORM-3 parent compound has been determined several times under various conditions and at different temperatures. Motterlini described a half-life for CORM-3 of 98 h in distilled water and of 3.6 min in blood plasma at 37 °C and less than 1 min in the presence of myoglobin (see the Supporting Information, Table S2).[18] Motterlini et al. used a separated chamber system which divided the CO releaser from the myoglobin.[15] McLean et al. reported that the CO release from CORM-2 and CORM-3 depended on myoglobin and was facilitated by an increasing concentration of the reducing agent sodium dithionite.[21] Furthermore, a loss of carbon monoxide was shown when CORM-3 was preincubated with sodium dithionite in the absence of myoglobin. After reduction of the myoglobin and removal of the sodium dithionite in the assay, no liberation of CO from CORM-3 was seen.[21] Santos-Silva et al. concluded that the interactions of CORM-3 with proteins result in the loss of a chloride ion, glycinate, and one CO ligand because of rapid formation of stable protein-Ru(CO_2) adducts.[23]

This may lead to several possible explanations of our half-life variations from **3** over **4c-500@3** to alginate@**4c-500@3** (Table 1). While the half-life increase from **3** (9 ± 1 min at 37 °C) to **4c-500@3** (65 ± 5 min at 37 °C) can be explained by decreasing interaction with myoglobin and sodium dithionite, the cause of the further increase to alginate@**4c-500@3** (172 ± 27 min at 37 °C) is not immediately clear. The latter increase might derive from the additional alginate diffusion barrier for CO out of and sodium dithionite or myoglobin into the alginate sphere. Therefore, additional experiments were carried out to elucidate the role of the alginate shell.

For alginate@CORM-3 spheres prepared in doubly deionized water, we determined a half-life of 106 ± 30 min at 37 °C with the myoglobin assay (MOPS buffer, myoglobin, $Na_2S_2O_4$) in the solution surrounding the alginate sphere (see the Supporting Information, Figure S17). The same alginate@CORM-3 spheres prepared with MOPS buffer solution inside the alginate spheres leads to a decreased half-life of 28 ± 8 min at 37 °C (see the Supporting Information, Figure S18). This agrees with trends in the literature[18] with a longer half-life for CORM-3 in distilled water than in buffered solutions (see the Supporting Information, Table S2). Determination of a half-life of alginate@CORM-3 with sodium dithionite inside the alginate spheres was not possible. Sodium dithionite led to rapid CO release from CORM-3 upon alginate-sphere preparation, and most of the CO was released until the spheres

DOI: 10.1021/acs.inorgchem.5b01675
Inorg. Chem. 2015, 54, 11236−11246

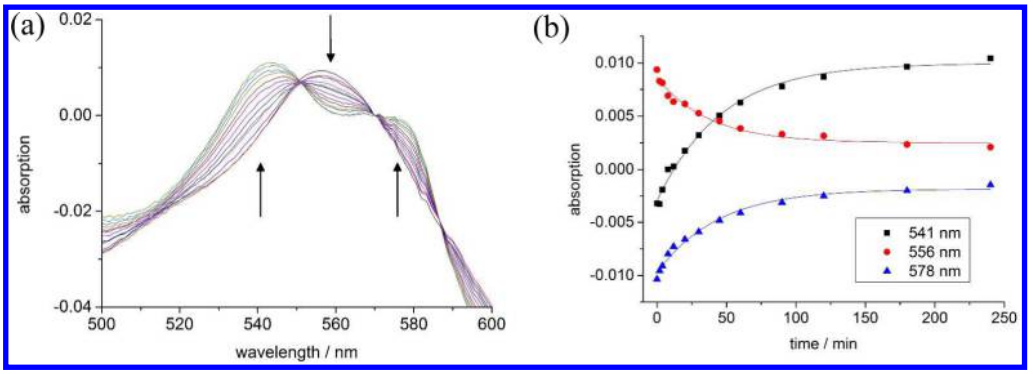

Figure 11. (a) Example for visible spectral changes in the myoglobin assay of the alginate@**4c-500@3** spheres with AC magnetic field at 50 °C. Visible spectra and absorption versus time plots for the other temperatures and without AC field are given in Figures S11−S16 in the Supporting Information Without the separation between black IONPs and myoglobin assay by alginate spheres, the UV/vis spectra are of much lower quality from which it is difficult to obtain the changes in absorption with good accuracy (see Figures S6−S8 in the Supporting Information).

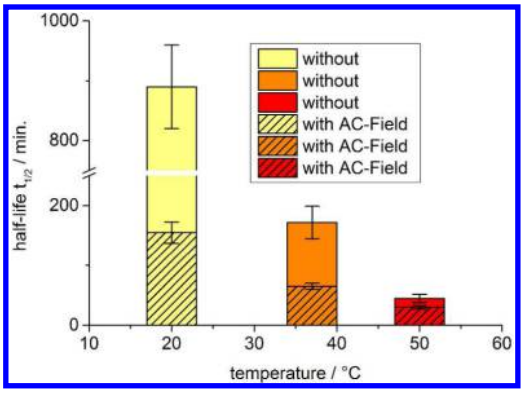

Figure 12. Half-life of CO release from alginate@**4c-500@3** spheres with and without AC field at different temperatures. The given temperatures of 20, 37, and 500 °C are the set solution temperatures also for the AC field. Note the broken *y*-axis for better visibility of the AC-field effect at 50 °C.

Table 1. Measured Half-Lives for CO Release Followed by Myoglobin Assay for Different Composite Compounds at 37 °C

composite compound[a]	half-life ($t_{1/2}$) [min]
CORM@IONP (**3**)[b]	9 ± 1
4c-500@3	65 ± 5
alginate@**4c-500@3** (∼2 mm spheres)[c]	172 ± 27
alginate@**4c-500@3** (∼1 mm spheres)[d]	100 ± 20
alginate@CORM-3 (d.d. H_2O inside)[e]	106 ± 30
alginate@CORM-3 (buffer inside)[f]	28 ± 8
alginate@CORM-3 ($Na_2S_2O_4$ inside)[g]	< ∼1[h]

[a]To determine the half-life of CO release by visible spectroscopy, the composite compound was immersed in the myoglobin solution with MOPS buffer and $Na_2S_2O_4$. [b]Value taken from the literature.[40] [c]Alginate spheres (Ø = 2 mm) containing MOPS buffer also inside. [d]Alginate spheres (Ø = 1 mm) containing MOPS buffer also inside. [e]Alginate spheres (Ø = 2 mm) containing doubly deionized (d.d.) H_2O. [f]Alginate spheres (Ø = 2 mm) containing MOPS buffer also inside. [g]Alginate spheres (Ø = 2 mm) containing the same concentration of $Na_2S_2O_4$ as the surrounding myoglobin/MOPS buffer/$Na_2S_2O_4$ solution. [h]Estimate because CO release was too rapid for measurement. Before alginate sphere preparation and transfer to UV/vis cell with myoglobin assay was complete, most of the CO was already released.

could be transferred into the UV/vis cell. McLean et al. described the important role of sodium dithionite for induced release of carbon monoxide from CORMs.[21] We can conclude that the alginate shell presents a diffusion barrier for MOPS buffer and especially for $Na_2S_2O_4$.

Our system of separating the CORM from the myoglobin assay shows a similar trend to the separated-chamber method of Motterlini.[18] The results from alginate@CORM-3 with and without MOPS buffer exclude a significant effect of the alginate shell on CO diffusion. If CO diffusion would be strongly hampered by the alginate shell, then there should not have been such a large decrease in half-life with MOPS buffer added to the alginate content. Instead, it is evident that the alginate shell slows the buffer and dithionite diffusion inside the spheres. The half-life of 28 ± 8 min at 37 °C for alginate@CORM-3 with MOPS buffer in comparison to 1 min for unprotected CORM-3 in the presence of the full myoglobin assay[20] is due to the alginate shell preventing the interaction between sodium dithionate and CORM-3. We assume no diffusion of myoglobin molecules into the alginate spheres because of the size of the protein. However, we have seen a decrease of the half-life with smaller compared to larger alginate spheres (∼1 mm versus ∼2 mm diameter) of alginate@**4c-500@3** (100 ± 20 min versus 172 ± 27 min at 37 °C) (see the Supporting Information, Figure S19). This effect correlates with the higher surface-to-volume ratio of the smaller spheres with the same total amount of **4c-500@3**. A higher surface area will allow for faster diffusion of the dithionite reducing agent through the ionic Ca-alginate shell. It is evident that the inclusion of MOPS buffer components at different amounts inside the alginate sphere can be used to fine-tune the half-life of CO release from the CORM.

To evaluate the surface temperature of the IONP reached by the AC field, we can use the plot of $t_{1/2}$ versus temperature or of $\ln(t_{1/2})$ versus temperature with the later being a straight line for higher accuracy (Figure 13). If we assume that, for an identical system, the half-life is solely a function of temperature, then the $\ln(t_{1/2})$ values reached under the AC magnetic field correspond to IONP surface temperatures of 37, 46, and 54 °C, up from the set solution temperatures of only 20, 37, and 50 °C, respectively (Figure 13a). A determination of the activation energy E_A with an Arrhenius plot of $\ln(\ln(2)/t_{1/2})$ versus $1/T$ gives a value of 78 kJ/mol (AC off) (Figure 13b). To the best of our knowledge, we found no activation energy for the CO release from a CORM in the literature.

DOI: 10.1021/acs.inorgchem.5b01675
Inorg. Chem. 2015, 54, 11236−11246

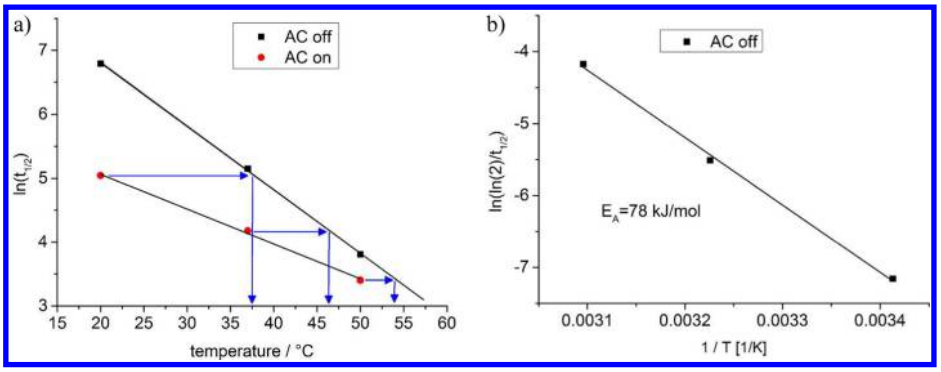

Figure 13. (a) Correlation of $\ln(t_{1/2})$ versus temperature for AC on and off to estimate the IONP surface temperature upon magnetic heating under the assumption of a direct correlation between half-life time and temperature. The initial temperature position of the red dots (AC on) is the set solution temperature. The AC field then leads to a higher temperature on the IONP surface which is traced by the blue arrows. (b) Arrhenius plot of $\ln k = \ln(\ln(2)/t_{1/2})$ versus $1/T_{Kelvin}$ to determine the activation energy from the slope ($-E_A/R$; R = 8.314 J mol^{-1} K^{-1}) of the graph.

Table 2. Cytotoxicity of Test Compounds and Cisplatin against the Human Ovarian Cancer Cell Line A2780, the Human Tongue Cancer Cell Line Cal27, and the Noncancer Cell Line HEK293[a,c]

	cell line					
	A2780		Cal27		HEK293	
compound	100 μM	10 μM	100 μM	10 μM	100 μM	10 μM
cisplatin	93.2		95.2		94.3	
CORM-2	0	0	20.8	0	13.9	9.23
CORM-3	5.20	5.73	22.0	2.25	18.0	7.04
5[b]	6.53	0	27.3	0	15.5	6.76
		100 μg/mL	10 μg/mL	100 μg/mL	10 μg/mL	100 μg/mL	10 μg/mL
Dextran@CORM@IONP (**4c-500@3**)		3.87	2.93	0	4.77	1.83	3.47

[a]Values are the mean of experiments performed in triplicate. [b]$PhCH_2CH(NH_2)CO_2RuCl(CO)_3$ (**5**, Figure S1). [c]The inhibition of cell growth is expressed as % of untreated control.

Dextran@CORM@IONP (**4c-500@3**) showed no significant cytotoxic effects (Table 2) up to 100 μg/mL (less than 4.77% growth inhibition) against the three cell lines A2780, Cal27, and HEK293 (see the Supporting Information, Figures S21−S24). The three reference compounds CORM-2, CORM-3, and $PhCH_2CH(NH_2)CO_2RuCl(CO)_3$ (**5**, Figure S1) showed very low cytotoxic effects between 2.25% and 9.23% growth inhibition at 10 μM. In a concentration of 100 μM, moderate growth inhibition of up to 27.3% was observed. For comparison, 100 μM cisplatin inhibited cell growth by >93%.

CONCLUSION

We present here a method of increasing the half-life and solubility of a kinetically unstable CORM-3 analogue, which has a short half-life in the presence of the myoglobin assay, as well as a new method to measure high UV/vis-absorbing CORMs in the myoglobin assay. In addition, the CORM was supported on maghemite (Fe_2O_3) iron oxide nanoparticles (IONP) to trigger the CO release by magnetic heating of the IONP instead of heating the surrounding solution. To achieve the desired and necessary water solubility, the CORM@IONP was surrounded by a water-soluble polymer. Dextran with a molar mass of 500 000 g/mol showed the best results in terms of water dispersibility together with CORM stabilization compared to Dextran with a lower molar mass of only 100 000 g/mol and PEG or PDADMAC. The composite Dextran@CORM@IONP led to an increase in half-life, $t_{1/2}$, to 58 ± 9 min at 20 °C compared to CORM@IONP with $t_{1/2}$ = 13 ± 2 min because the CORM-3 analogue became protected from rapid CO-displacement reactions with the myoglobin-assay components (protein, MOPS buffer, $Na_2S_2O_4$). Second, the dark-colored Dextran@CORM@IONP composite with high UV/vis absorptivity was separated from the myoglobin assay by compartmentation in alginate. Consequently, the UV/vis spectral changes of the myoglobin assay in the solution outside of the alginate spheres could be observed without interference of the dark-colored CORM@IONP composite. The ability to measure high absorbing substances in the well-known and frequently used myoglobin assay standard test in a simple UV/vis cell with low costs is a huge benefit compared to other methods. Half-life measurements for CO release from alginate@Dextran@CORM@IONP composites then supported the proof-of-concept for CO release by magnetic heating of CORM@IONP. We could show that the half-life for CO release from CORM@IONP in the alginate@Dextran shell could be triggered and lowered by a factor of ~2.6 (from 172 ± 27 min to 65 ± 5 min) at the physiological temperature of 37 °C upon magnetic heating in an alternating current magnetic field (31.7 kA m^{-1}, 247 kHz, 39.9 mT). At 20 °C, the half-life decreased 5.7 times at 50 °C, 1.5 times upon magnetic heating of the alginate@Dextran@CORM@IONP composites. The decrease in half-life could be correlated to the increased surface temperature of the IONP reached with magnetic heating. From temperature-variable kinetic measurements, an activation energy of 78 kJ/mol was determined for the CO release from the IONP-surface bound CORM-3 analogue, IONP(μ-O)$_2$-$C_6H_3CH_2CH(NH_2)CO_2$-$\kappa N,O$-$RuCl(CO)_3$ The alginate method presented here is not limited to substitution labile substances. It could also be used to measure photolabile CORMs whose absorption bands overlap with the myoglobin

DOI: 10.1021/acs.inorgchem.5b01675
Inorg. Chem. 2015, 54, 11236−11246

bands. Altogether, we illustrated new ways for increasing the half-life of CORMs for more controlled CO release and methods for measuring the CO release from samples with high absorptivity.

EXPERIMENTAL SECTION

All chemicals were purchased from Acros, Aldrich, VWR, and Fluka and used as received. $[Ru(CO)_3Cl_2]_2$ was synthesized according to literature procedures.[60] Doubly deionized (d.d.) water was obtained by a Millipore Synergy with a conductivity of 0.05 μS/cm.

IR Spectra. IR spectra were recorded on a Bruker Tensor 37 IR-spectrometer with KBr discs. IR spectroscopic measurements of the black-colored CORM@IONP (**3**) in attenuated total reflectance (ATR) mode gave only very small signal intensities. After optimization, IR spectra of CORM@IONP (**3**) were obtained as KBr discs. For this, the functionalized nanoparticles **2**, **3**, and **4** were ground for a prolonged time with dry KBr to achieve a fine distribution. Care was taken to keep the CORM@IONP (**3**) concentration low (1−2 mg/30−50 mg KBr) because of strong absorption bands. The integration time was set to 50 scans per wavenumber to obtain good quality spectra. The IR analysis of the different compounds is given in the Supporting Information.

Scanning Transmission Electron Micrographs (STEM). Micrographs were obtained with a FEI Titan 80-300 TEM at Ernst-Ruska Centrum (ER-C) of Forschungszentrum (FZ) Jülich. For the sample preparation, about 1 mg of the particles was dispersed by sonication and fast up-and-down pipetting in a 1 mL syringe in deionized water (2 mL). This dispersion was diluted 1:10 with deionized water to yield a very low concentration of the nanoparticles. One drop of this dispersion was placed on a holey thin film of amorphous carbon on a copper grid. After a contact time of 15 min, the grid was floated on a water surface and held vertically to rinse off the solvent.

Dynamic Light Scattering Measurements. DLS measurements were done in a Malvern Zetasizer Nanoseries. For the determination of the IONP (**1**), DOPA@IONP (**2**), and **4c-500@3** nanoparticles size distribution, a solution with a minimum concentration of 1 mg/mL in doubly deionized water was prepared. Measurement at different concentrations of the dispersion yielded the same hydrodynamic diameter.

Atom Absorption Measurements (AAS). AAS measurements for ruthenium and iron were carried out with a PerkinElmer AAS AAnalyst200 by MicroLab Kolbe, Höhenweg 17, D-45470 Mülheim, Germany.

UV/vis Absorption Spectra. Spectra were collected on a Specord S 600 UV/vis spectrometer from Analytik Jena Co. This work was carried out under nitrogen or argon and with thermostated cuvettes.

AC Field Generator. Measurements were done with a Hüttinger HF generator AXIO T5, equipped with a water-cooled copper induction coil. The system was operated at 247 kHz, with a magnetic field amplitude of 31.7 kA/m^{-1} and 39.9 mT.

Synthesis. *Synthesis of Maghemite (γ-Fe_2O_3) Nanoparticles IONP (**1**).* Maghemite nanoparticles were prepared following a known literature procedure (see the Supporting Information).[40,61]

*Synthesis of DOPA@IONP (**2**).* A 300 mg portion of **1** was dispersed in 100 mL of doubly deionized water. 160 mg of DOPA (D,L-3,4-dihydroxyphenyl-alanine) was dissolved in a small amount of water with ultrasound before the two solutions were combined and the pH value was adjusted to 7.6 using NaOH. After addition of 800 mL of acetone, the particles were sedimented and collected with a permanent magnet and the supernatant was discarded. The particles were washed three times with acetone and dried overnight under vacuum. Yield: 192 mg.

*Synthesis of CORM@IONP (**3**).* A 20 mg portion of **2** and 20 mg (45 mmol) of $[Ru(CO)_3Cl_2]_2$ were separately dissolved in water in an ultrasonic bath. The two solutions were combined and stirred for 3 h at room temperature. After adding acetone, the particles were sedimented with a permanent magnet and the supernatant was discarded. The particles were washed three times with acetone and dried overnight under vacuum. Yield: 17.7 mg.

*General Synthesis of Poly@CORM@IONP (**4**).* A 20 mg portion of DOPA-coated nanoparticles, 20 mg (45 mmol) of $[Ru(CO)_3Cl_2]_2$, and 60 mg of polymer were separately dissolved in water in an ultrasonic bath. The three solutions were combined (final volume: about 10 mL) and stirred for 3 h at room temperature. After adding 10 mL of acetone, the particles were sedimented with a permanent magnet and the supernatant was discarded. Finally, the particles were washed three times with acetone and dried overnight under vacuum. Yields and IR analysis of the different hybrid compounds **4** are given in the Supporting Information.

*Synthesis of Alginate@**4c-500@3**.* A 10 mg portion of **4c-500@3** was dissolved in 0.5 mL of MOPS buffer (pH 7.4). Mixing of 0.3 mL of this solution with 0.7 mL of alginate solution (50 mg sodium alginate in 10 mL of d.d. water) leads to a viscous solution, which was added dropwise (by B-Braun, Sterican, 0.60 × 80 mm BL/LB) into a calcium chloride solution (2 g of $CaCl_2 \cdot 6H_2O$ in 60 mL of d.d. water). The resulting spheres were left for 30 min in the calcium chloride solution to form a fully cross-linked network of the alginate. Then, the formed spheres were washed three times each with 10 mL of MOPS buffer and stored in the solution.

Myoglobin Assay. *MOPS Buffer 0.1 mol/L pH 7.4.* A 2.09 g (0.01 mol) portion of 3-(*N*-morpholino)propanesulfonic acid (MOPS) was dissolved in 75 mL of water. Subsequently, the pH was adjusted to 7.4 using NaOH and water was added to reach a final volume of 100 mL.

*Myoglobin Assay with Poly@CORM@IONP (**4**).* A 5.0 mg (0.29 μmol) portion of myoglobin from equine heart muscle was dissolved in 3.25 mL of MOPS buffer at pH 7.4 and degassed by bubbling nitrogen or argon through the solution. Subsequently, 30 mg (0.17 mmol, excess 550×) of sodium dithionite ($Na_2S_2O_4$) was added in order to obtain desoxymyoglobin. MOPS buffer at pH 7.4 was also degassed with inert gas. In a small flask, 1.2 mg of sample was dissolved in 1.4 mL of MOPS buffer at pH 7.4 through fast pipetting up and down in a 1 mL syringe. 0.6 mL of dissolved sample and 0.6 mL of degassed MOPS buffer at 7.4 were filled into a thermostatable quartz cuvette under inert gas before 0.2 mL of the myoglobin stock solution was added to reach a final volume of 1.4 mL (cuvette concentrations: 12.8 μmol/L myoglobin, 7.04 mmol/L sodium dithionite). A reference was prepared from 0.8 mL of buffer and 0.6 mL of sample solution. The measurement was started subsequently in the range of 500−600 nm after sealing the two cuvettes and mounting them to the thermostat. In order to ensure reliability, all sample data were collected at least 3 times.

*Myoglobin Assay with Alginate@**4c-500@3**.* A 5.0 mg (0.29 μmol) portion of myoglobin from equine heart muscle was dissolved in 7 mL of MOPS buffer (pH 7.4) and degassed from dioxygen by bubbling nitrogen or argon through the solution. Subsequently, 30 mg (0.17 mmol, excess 550×) of sodium dithionite was added in order to obtain desoxymyoglobin. MOPS buffer pH 7.4 was also freed from dioxygen with inert gas. The number of 15 alginate spheres and 0.6 mL of degassed MOPS buffer (pH 7.4) were filled into a thermostated quartz cuvette under inert gas before 0.2 mL of the myoglobin stock solution was added to reach a final volume of 1.4 mL (cuvette concentrations: 12.8 μmol myoglobin, 7.04 mmol/L sodium dithionite). The visible absorption measurement was started in the range of 500−600 nm after sealing the cuvette and mounting it in the thermostat. In order to ensure reliability, every data set was collected at least three times at each temperature.

Toxicity Tests. *Biological Evaluation.* Reagent Cisplatin was purchased from Sigma-Aldrich (Germany), and 3-(4,5-dimethylthiazol-2-yl)-2,5-diphenyltetrazolium bromide (MTT) was purchased from Serva (Germany). All other reagents were supplied by PAN Biotech (Germany) unless otherwise stated.

Cell Lines and Cell Culture. The human epithelial ovarian cancer cell line A2780 was obtained from the European Collection of Cell Cultures (ECACC, U.K.). The human tongue cell line Cal27 and the human embryonic kidney cell line HEK293 were obtained from the German Collection of Microorganisms and Cell Cultures (DSMZ, Germany). All cell lines were grown at 37 °C in a humidified atmosphere containing 5% CO_2 in RPMI 1640 (A2780) or DMEM (Cal27, HEK293) containing 10% fetal calf serum, 120 IU/mL

DOI: 10.1021/acs.inorgchem.5b01675
Inorg. Chem. 2015, 54, 11236−11246

penicillin, and 120 μg/mL streptomycin. The cells were grown to 80% confluency before using them for the appropriate assays.

MTT Cell Viability Assay. The rate of cell survival under the action of test compounds was evaluated by an improved MTT assay as previously described.[62] In brief, A2780, Cal27, or HEK293 were seeded at a density of 5000 (A2780) or 2000 (Cal27, HEK293) cells/well in 96-well plates (Corning, Germany). After 24 h, cells were exposed to increased concentrations of test compounds. Incubation was ended after 72 h, and cell survival was determined by addition of MTT solution (5 mg/mL in phosphate buffered saline). The formazan precipitate was dissolved in DMSO (VWR, Germany). Absorbance was measured at 544 and 690 nm in a FLUOstar microplate-reader (BMG LabTech, Germany).

■ ASSOCIATED CONTENT

Supporting Information

The Supporting Information is available free of charge on the ACS Publications website at DOI: 10.1021/acs.inorgchem.5b01675.

Details of synthesis, IR characterization, TEM images, time-dependent visible absorption spectra, plots of the intensity changes of selected wavelengths, and bar diagrams of toxicity tests (PDF)

■ AUTHOR INFORMATION

Corresponding Author

*E-mail: janiak@uni-duesseldorf.de.

Notes

The authors declare no competing financial interest.
E-mail: annette.schmidt@uni-koeln.de (A.M.S.).
E-mail: matthias.kassack@hhu.de (M.U.K.).

■ ACKNOWLEDGMENTS

We thank Dr. Juri Barthel and the Ernst Ruska-Centre (ER-C) for Microscopy and Spectroscopy with Electrons, Jülich Research Centre, and RWTH Aachen University, 52425 Jülich (Germany) for help and access to the HR-TEM facilities. We also thank the referees for their valuable and helpful comments.

■ REFERENCES

(1) Haldane, B. J. *Biochem. J.* **1927**, *21*, 1068−1075.
(2) Prockop, L. D.; Chichkova, R. I. *J. Neurol. Sci.* **2007**, *262*, 122−130.
(3) Johnson, T. R.; Mann, B. E.; Clark, J. E.; Foresti, R.; Green, C. J.; Motterlini, R. *Angew. Chem., Int. Ed.* **2003**, *42*, 3722−3729.
(4) Tenhunen, R.; Marver, H. S.; Schmid, R. *Proc. Natl. Acad. Sci. U. S. A.* **1968**, *61*, 748−755.
(5) Boehning, D.; Snyder, S. H. *Science* **2002**, *298*, 2339−2340.
(6) Motterlini, R.; Otterbein, L. E. *Nat. Rev. Drug Discovery* **2010**, *9*, 728−743.
(7) Mann, B. E. *Organometallics* **2012**, *31*, 5728−5735.
(8) Carpenter, A. W.; Schoenfisch, M. H. *Chem. Soc. Rev.* **2012**, *41*, 3742−3752.
(9) Bredt, D. S.; Snyder, S. H. *Annu. Rev. Biochem.* **1994**, *63*, 175−195.
(10) Mann, B. E.; Motterlini, R. *Chem. Commun.* **2007**, 4197−4208.
(11) Foresti, R.; Motterlini, R. *Curr. Drug Targets* **2010**, *11*, 1595−1604.
(12) Ryter, S. W.; Alam, J.; Choi, A. M. K. *Physiol. Rev.* **2006**, *86*, 583−650.
(13) Wareham, L. K.; Poole, R. K.; Tinajero-Trejo, M. *J. Biol. Chem.* **2015**, *290* (31), 18999−19007.
(14) Clark, J. E.; Naughton, P.; Shurey, S.; Green, C. J.; Johnson, T. R.; Mann, B. E.; Foresti, R.; Motterlini, R. *Circ. Res.* **2003**, *93*, e2−e8.
(15) Motterlini, R.; Clark, J. E.; Foresti, R.; Sarathchandra, P.; Mann, B. E.; Green, C. J. *Circ. Res.* **2002**, *90*, e17−e24.
(16) Seixas, J. D.; Santos, M. F. A.; Mukhopadhyay, A.; Coelho, A. C.; Reis, P. M.; Veiros, L. F.; Marques, A. R.; Penacho, N.; Goncalves, A. M. L.; Romao, M. J.; Bernardes, G. J. L.; Santos-Silva, T.; Romao, C. C. *Dalton Trans.* **2015**, *44*, 5058−5075.
(17) Oresmaa, L.; Tarvainen, H.; Machal, K.; Haukka, M. *Dalton Trans.* **2012**, *41*, 11170−11175.
(18) Motterlini, R.; Mann, B. E.; Johnson, T. R.; Clark, J. E.; Foresti, R.; Green, C. J. *Curr. Pharm. Des.* **2003**, *9*, 2525−2539.
(19) Alberto, R.; Motterlini, R. *Dalton Trans.* **2007**, 1651−1660.
(20) Motterlini, R.; Mann, B. E.; Foresti, R. *Expert Opin. Invest. Drugs* **2005**, *14*, 1305−1318.
(21) McLean, S.; Mann, B. E.; Poole, R. K. *Anal. Biochem.* **2012**, *427*, 36−40.
(22) Johnson, T. R.; Mann, B. E.; Teasdale, I. P.; Adams, H.; Foresti, R.; Green, C. J.; Motterlini, R. *Dalton Trans* **2007**, 1500−1508.
(23) Santos-Silva, T.; Mukhopadhyay, A.; Seixas, J. D.; Bernardes, G. J. L.; Romao, C. C.; Romao, M. J. *J. Am. Chem. Soc.* **2011**, *133*, 1192−1195.
(24) García-Gallego, S.; Bernardes, G. J. L. *Angew. Chem., Int. Ed.* **2014**, *53*, 9712−9721.
(25) Tavares, A. F. N.; Teixeira, M.; Romao, C. C.; Seixas, J. D.; Nobre, L. S.; Saraiva, L. M. *J. Biol. Chem.* **2011**, *286*, 26708−26717.
(26) Pitchumony, T.; Spingler, B.; Motterlini, R.; Alberto, R. *Chimia* **2008**, *62*, 277−279.
(27) Motterlini, R.; Sawle, P.; Hammad, J.; Bains, S.; Alberto, R.; Foresti, R.; Green, C. J. *Pharmacol. Res.* **2005**, *19*, 284−286.
(28) Brückmann, N. E.; Wahl, M.; Reiß, G. J.; Kohns, M.; Wätjen, W.; Kunz, P. C. *Eur. J. Inorg. Chem.* **2011**, *2011*, 4571−4577.
(29) Huber, W.; Linder, R.; Niesel, J.; Schatzschneider, U.; Spingler, B.; Kunz, P. C. *Eur. J. Inorg. Chem.* **2012**, *2012*, 3140−3146.
(30) Romanski, S.; Kraus, B.; Schatzschneider, U.; Neudörfl, J. M.; Amslinger, S.; Schmalz, H. G. *Angew. Chem.* **2011**, *123*, 2440−2444.
(31) Ma, M.; Noei, H.; Mienert, B.; Niesel, J.; Bill, E.; Muhler, M.; Fischer, R. A.; Wang, Y.; Schatzschneider, U.; Metzler-Nolte, N. *Chem. - Eur. J.* **2013**, *19*, 6785−6790.
(32) Dördelmann, G.; Meinhardt, T.; Sowik, T.; Krueger, A.; Schatzschneider, U. *Chem. Commun.* **2012**, *48*, 11528−11530.
(33) Ruggi, A.; Zobi, F. *Dalton Trans.* **2015**, *44*, 10928−10931.
(34) Bohlender, C.; Glaser, S.; Klein, M.; Weisser, J.; Thein, S.; Neugebauer, U.; Popp, J.; Wyrwa, R.; Schiller, A. *J. Mater. Chem. B* **2014**, *2*, 1454−1463.
(35) Schatzschneider, U. *Br. J. Pharmacol.* **2015**, *172*, 1638−1650.
(36) Matsumura, Y.; Maeda, H. *Cancer Res.* **1986**, *46*, 6387−6392.
(37) Maeda, H.; Wu, J.; Sawa, T.; Matsumura, Y.; Hori, K. *J. Controlled Release* **2000**, *65*, 271−284.
(38) D'Andrea, L. D.; Romanelli, A.; Di Stasi, R.; Pedone, C. *Dalton Trans.* **2010**, *39*, 7625−7636.
(39) Neuse, E. *Metal-Based Drugs* **2008**, *2008*, 1−19.
(40) Kunz, P. C.; Meyer, H.; Barthel, J.; Sollazzo, S.; Schmidt, A. M.; Janiak, C. *Chem. Commun.* **2013**, *49*, 4896−4898.
(41) Lee, N.; Hyeon, T. *Chem. Soc. Rev.* **2012**, *41*, 2575−2589.
(42) Elsabahy, M.; Wooley, K. L. *Chem. Soc. Rev.* **2012**, *41*, 2545−2561.
(43) Girginer, B.; Galli, G.; Chiellini, E.; Bicak, N. *Int. J. Hydrogen Energy* **2009**, *34*, 1176−1184.
(44) Koneracka, M.; Antošová, A.; Zavisova, V.; Lancz, G.; Gazova, Z.; Siposova, B. K.; Jurikova, A.; Csach, K.; Kovac, J.; Tomasovicova, N. *Acta. Phys. Polym.* **2010**, *118*, 983−985.
(45) Tassa, C.; Shaw, S. Y.; Weissleder, R. *Acc. Chem. Res.* **2011**, *44*, 842−852.
(46) Schatzschneider, U. *Eur. J. Inorg. Chem.* **2010**, *2010*, 1451−1467.
(47) Atkin, A. J.; Lynam, J. M.; Moulton, B. E.; Sawle, P.; Motterlini, R.; Boyle, N. M.; Pryce, M. T.; Fairlamb, I. J. S. *Dalton Trans.* **2011**, *40*, 5755−5761.
(48) Klein, M.; Neugebauer, U.; Gheisari, A.; Malassa, A.; Jazzazi, T. M.; Froehlich, F.; Westerhausen, M.; Schmitt, M.; Popp, J. *J. Phys. Chem. A* **2014**, *118*, 5381−5390.

DOI: 10.1021/acs.inorgchem.5b01675
Inorg. Chem. 2015, 54, 11236−11246

(49) Yuan, L.; Lin, W. Y.; Tan, L.; Zheng, K. B.; Huang, W. M. *Angew. Chem., Int. Ed.* **2013**, *52*, 1628−1630.
(50) Michel, B. W.; Lippert, A. R.; Chang, C. J. *J. Am. Chem. Soc.* **2012**, *134*, 15668−15671.
(51) Vreman, H. J.; Stevenson, D. K. *Anal. Biochem.* **1988**, *168*, 31−81.
(52) Balazy, M.; Jiang, H. *Acta Haematol.* **2000**, *103*, 78.
(53) Draget, K. I. Alginates. In *Handbook of Hydrocolloids*; Phillips, G. O., Williams, P. A., Eds.; Boca Raton: FL, 2009; pp 379−95.
(54) Pawar, S. N.; Edgar, K. J. *Biomaterials* **2012**, *33*, 3279−3305.
(55) Boateng, J. S.; Matthews, K. H.; Stevens, H. N. E.; Eccleston, G. M. *J. Pharm. Sci.* **2008**, *97*, 2892−923.
(56) Zimmermann, H.; Shirley, S.; Zimmermann, U. *Curr. Diabetes Rep.* **2007**, *7*, 314−320.
(57) Lee, K. Y.; Mooney, D. J. *Prog. Polym. Sci.* **2012**, *37*, 106−126.
(58) Barham, P.; Skibsted, L. H.; Bredie, W. L. P.; Frøst, M. B.; Møller, P.; Risbo, J.; Snitkjaer, P.; Mortensen, L. M. *Chem. Rev.* **2010**, *110* (4), 2313−2365.
(59) Spjelkavik, A. I.; Aarti; Divekar, S.; Didriksen, T.; Blom, R. *Chem.-Eur. J.* **2014**, *20*, 8973−8978.
(60) Mantovani, A.; Cenini, S.; Heintz, R. M.; Morris, D. E. *Inorg. Synth.* **1976**, *16*, 51−53.
(61) van Ewijk, G. A.; Vroege, G. J.; Philipse, A. P. *J. Magn. Magn. Mater.* **1999**, *201*, 31−33.
(62) Marek, L.; Hamacher, A.; Hansen, F. K.; Kuna, K.; Gohlke, H.; Kassack, M. U.; Kurz, T. *J. Med. Chem.* **2013**, *56* (2), 427−436.

DOI: 10.1021/acs.inorgchem.5b01675
Inorg. Chem. 2015, 54, 11236−11246